Pyrrolizin-3-one and its 1,2-dihydro derivative: structures of the free molecules determined by electron diffraction and *ab initio* calculations and in the crystal by X-ray diffraction †

Frank Blockhuys,‡[a] Sarah L. Hinchley,[a] Heather E. Robertson,[a] Alexander J. Blake,[b] Hamish McNab,[a] Xavier L. M. Despinoy,[a] Steven G. Harris[a] and David W. H. Rankin*[a]

[a] *Department of Chemistry, The University of Edinburgh, West Mains Road, Edinburgh, UK EH9 3JJ*
[b] *School of Chemistry, The University of Nottingham, University Park, Nottingham, UK NG7 2RD*

Received (in Cambridge, UK) 15th March 2001, Accepted 24th August 2001
First published as an Advance Article on the web 16th October 2001

The molecular structures of pyrrolizin-3-one **1** and 1,2-dihydropyrrolizin-3-one **2** have been investigated in the gas phase by *ab initio* calculations (both compounds) and electron diffraction using the SARACEN method of structural analysis (parent compound only), and in the solid phase at 150 K by low-temperature X-ray diffraction. Important structural parameters (r_{h1} structure) for a free molecule of **1** are: *r*(C–O) 1.215(4) and *r*[N–C(CO)] 1.437(4) Å. For **2** these (r_e structure) are: *r*(C–O) 1.2095 and *r*[N–C(CO)] 1.4068 Å. The corresponding values in the crystal for **1** are *r*(C–O) 1.207(2) and *r*[N–C(CO)] 1.408(2) Å, and for **2** *r*(C–O) 1.216(2) and *r*[N–C(CO)] 1.392(2) Å.

Introduction

Pyrrolizin-3-one **1** possesses an unusual conjugated system in which the normal amide resonance creates a formally anti-aromatic canonical form **1a** (Scheme 1).[1] In contrast, 1,2-dihydropyrrolizin-3-one **2** is structurally a simple cyclic *N*-acylated pyrrole with no possibility of complete cyclic electron delocalisation. We have previously probed the structures of these (and related) ring systems by X-ray crystallography using the 6-bromo compound **3**[2] and the pyrrolo[1,2-*c*]imidazol-5-ones (azapyrrolizinones) **4** and **5**[3] as model compounds. These studies suffered from the disadvantage of the presence of either a heavy atom or of an additional ring heteroatom, and so we report here a comprehensive structural study of pyrrolizin-3-one **1** itself. Because this compound is a liquid at room temperature, we grew a crystal and collected X-ray diffraction data at low temperature in order to establish its solid state structure. The compound is also fairly volatile, so the gas-phase structure was also determined experimentally by gas electron diffraction (GED) (using the SARACEN, structure analysis restrained by *ab initio* calculations for electron diffraction,[4] method) and theoretically by high level *ab initio* calculations. For comparison, we also report the crystal and calculated gas-phase structure of 1,2-dihydropyrrolizin-3-one **2**.

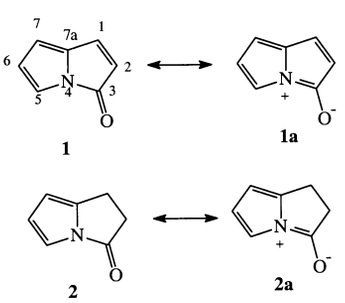

Scheme 1

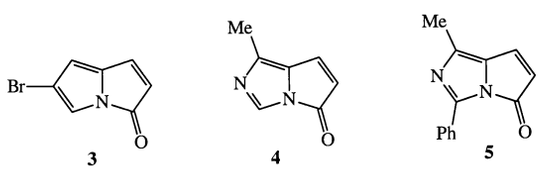

Experimental

Synthesis

Pyrrolizin-3-one **1** was synthesised by flash vacuum pyrolysis of the condensation product of Meldrum's acid (2,2-dimethyl-1,3-dioxane-4,6-dione) and pyrrole-2-carbaldehyde as previously described.[5] The dihydro-derivative **2** was obtained by hydrogenation of **1** over Pd/C under mild conditions.[6] The purity of these compounds was confirmed by NMR methods.

FT-Raman spectra were recorded on a LabRam confocal microscope (Instruments S.A. Ltd.), using a 25 mW laser with excitation at 632.8 nm. FT-IR spectra were recorded on a Perkin Elmer Paragon 1000 instrument.

Electron diffraction measurements

Electron scattering intensities were recorded on Kodak Electron Image plates using the Edinburgh gas electron-diffraction apparatus,[7] operating at *ca.* 40 kV. Six plates (two from the long and four from the short camera distance) for **1** were recorded and converted into digital format using a computer controlled PDS microdensitometer at the Institute of Astronomy, Cambridge, employing a 200 μm pixel size.[8] Standard programs were used for the data reduction with the scattering factors of Ross *et al.*[9] Sample and nozzle temperatures, nozzle-to-plate distances *d*, weighting functions used to set up the off-diagonal weight matrix, correlation parameters, final scale factors *k* and electron wavelengths λ for the measurements are collected in Table 1.

† Electronic supplementary information (ESI) available: further experimental data. See http://www.rsc.org/suppdata/p2/b1/b102475m/
‡ *Present address*: Department of Chemistry, University of Antwerpen, Universiteitsplein 1, B-2610 Wilrijk, Belgium.

Table 1 Experimental parameters for GED analysis of **1**

d/mm	T_{sample} [a]	T_{nozzle} [a]	Δs [b]	s_{min} [b]	sw_1 [b]	sw_2 [b]	s_{max} [b]	corr. par.	*k*	λ/pm [c]
88.03	46	78	0.4	10.0	12.0	30.4	35.6	0.4586	0.905(39)	6.0155
256.91	87	100	0.2	2.0	4.0	13.0	15.2	0.4753	0.742(10)	6.0155

[a] In °C. [b] In Å^{-1}. [c] Determined by reference to the scattering patterns of benzene vapour.

X-Ray structure determination

Pyrrolizin-3-one **1**, a deep red liquid, was purified by Kugelrohr distillation and sealed in a fine Pyrex capillary tube using epoxy adhesive. The tube was fixed in a thermally insulating Tufnol pip, which was then mounted in a standard arcless goniometer head. The sample was mounted on a Stoe Stadi-4 four-circle diffractometer with χ set to −90 °, 10 mm from the outlet nozzle of an Oxford Cryosystems low-temperature device.[10] Solidification using liquid nitrogen followed by elevation of the temperature caused the sample to melt in the range 266–274 K. Controlled crystal growth was achieved by maintaining the sample at 265 K and interrupting the gas stream with a spatula placed between the sample and the nozzle. A section of the solid exhibited extinction in plane-polarised light at $\chi = 120 \pm 5°$ which indicated the presence of a single crystal.

Crystal data for 1. C_7H_5NO, M = 119.12, monoclinic, a = 13.960(5), b = 5.954(2), c = 14.181(5) Å, β = 104.42(4)°, V = 1141.6(7) Å^3, T = 150(2) K, space group $C2/c$ (No. 15), Z = 8, D_c = 1.386 g cm^{-3}, μ(Mo-Kα) = 0.095 mm^{-1}, 1674 unique reflections (R_{int} 0.020) measured and used in all calculations. Final R_1 [1342$F \geq 4\sigma(F)$] = 0.0531 and wR(all F^2) was 0.168.

Crystal data for 2. C_7H_7NO, M = 121.14, monoclinic, a = 6.629(5), b = 12.996(9), c = 7.373(5) Å, β = 109.78(5)°, V = 597.7(7) Å^3, T = 150(2) K, space group $P2_1/c$ (No. 14), Z = 4, D_c = 1.346 g cm^{-3}, μ(Mo-Kα) = 0.092 mm^{-1}, 1048 unique reflections (R_{int} 0.024) measured and used in all calculations. Final R_1 [914$F \geq 4\sigma(F)$] = 0.0340 and wR(all F^2) was 0.0937.

Geometry optimisations, frequency and force-field calculations

Ab initio and density functional theory (DFT) calculations on all compounds were performed using GAUSSIAN 98.[11] A graded series of calculations was performed for the parent compound **1** in order to gauge the effects of basis set size and electron correlation treatments on the optimised structures. The calculations were performed using standard gradient techniques at the HF level of theory using the 3-21G* basis set[12] and 6-31G* basis set[13] on all atoms, at the B3LYP level using 6-31G* on all atoms, at the B3LYP level with 6-31G* on H and 6-311+G* on N, O and C (ref. 14) and at the MP2 level using 6-31G* on H and 6-311+G* on N, O and C. The calculations for **2** were performed only at the B3LYP and MP2 levels with 6-31G* on H and 6-311+G* on N, O and C. Vibrational frequencies were calculated at the B3LYP/6-311+G* level (6-31G* on H) for both **1** and **2**. For **1** the force field described in Cartesian coordinates was transformed into one described by a set of pseudo-symmetry coordinates using the program ASYM40[15] and was then used to calculate the amplitudes of vibration, u, after scaling (see below). The definitions of the normal coordinates are listed in the supplementary data. Furthermore, perpendicular amplitudes of vibration, k, were corrected for shrinkage effects by treating the force field in terms of coordinates closely approximating the true curvilinear motions of the atoms in the molecule.[16] These k values allowed refinement of the r_{h1} structure, rather than r_{h0} ($\equiv r_a$), which is obtained using k values determined assuming rectilinear motions. (For definitions of r_{h0}, r_{h1}, *etc.*, see ref. 15.)

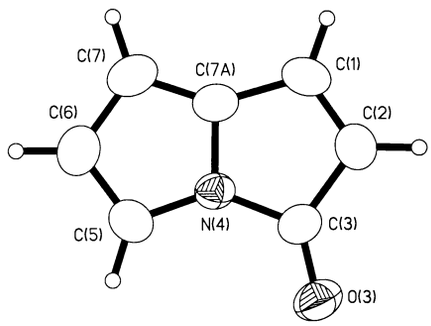

Fig. 1 Molecular structure and atomic numbering of pyrrolizin-3-one **1** in the crystal. Displacement ellipsoids are drawn at the 50% probability level and hydrogen atoms are shown as small circles of arbitrary radius.

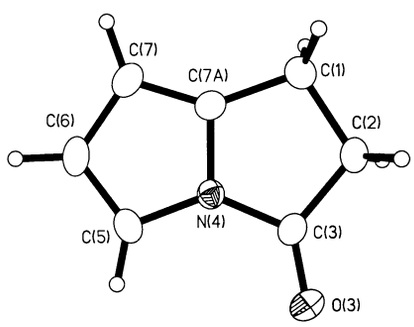

Fig. 2 Molecular structure and atomic numbering of 1,2-dihydropyrrolizin-3-one **2** in the crystal. Displacement ellipsoids are drawn at the 50% probability level and H atoms are shown as small circles of arbitrary radius.

Results and discussion

Ab initio calculations

The molecular framework and the atomic numbering of **1** and **2** used in the calculations are shown in Fig. 1 and 2 respectively; each hydrogen atom is assigned the same number as the carbon atom on which it is positioned. Force fields calculated at the B3LYP/6-311+G* level (6-31G* on H) confirmed that free molecules of both compounds have C_s symmetry. Table 2 shows the calculated geometries at the different levels of theory used in this study. The two DFT calculations for **1** display convincing agreement for all parameters, the largest differences in bond lengths and valence angles being about 0.006 Å and 0.2° respectively: introducing a triple-ζ basis set and diffuse functions on the heavy atoms seems to play a minor role in the expression of the geometry. As expected, the differences between DFT and MP2 are slightly larger and these can be found primarily in the C=C bonds, where the variations amount to 0.013, 0.013 and 0.009 Å for C(5)=C(6), C(7)=C(7a) and C(1)=C(2) respectively; the other bond lengths deviate by no more than 0.005 Å. This is reflected in the valence angles, for which the differences amount to about 0.6°. The calculations on **2** reflect a similar agreement between the two correlated methods used here, even though the differences for the C=C bonds are now somewhat larger, amounting to about 0.014 Å. The differences for the other bonds are limited to about half that value, and the variations in the valence angles are no larger

Table 2 Molecular geometries (r_e distances in Å and angles in °) calculated for **1** and **2** by a range of *ab initio* methods

	1				**2**	
Parameter	HF/6-31G*	B3LYP/6-31G*	B3LYP/6-311+G*	MP2/6-311+G*	B3LYP/6-311+G*	MP2/6-311+G*
N(4)–C(5)	1.3730	1.3807	1.3815	1.3813	1.3845	1.3801
N(4)–C(7a)	1.3705	1.3811	1.3804	1.3763	1.3892	1.3846
N(4)–C(3)	1.3977	1.4289	1.4301	1.4319	1.3995	1.4068
C(5)–C(6)	1.3523	1.3761	1.3738	1.3863	1.3706	1.3847
C(6)–C(7)	1.4469	1.4396	1.4397	1.4362	1.4416	1.4367
C(7)–C(7a)	1.3492	1.3771	1.3750	1.3875	1.3663	1.3800
C(1)–C(7a)	1.4681	1.4568	1.4554	1.4584	1.5035	1.5033
C(1)–C(2)	1.3300	1.3539	1.3516	1.3605	1.5517	1.5479
C(2)–C(3)	1.4996	1.4938	1.4921	1.4941	1.5306	1.5268
C(3)–O(3)	1.1851	1.2102	1.2046	1.2098	1.2045	1.2095
⟨=C–H⟩	1.0705	1.0817	1.0828	1.0862	1.0824	1.0856
⟨–C–H⟩	—	—	—	—	1.0961	1.0977
C(5)–N(4)–C(7a)	109.8	110.2	110.1	110.6	110.3	111.0
C(3)–N(4)–C(7a)	111.8	111.2	111.1	111.2	114.0	113.7
C(7)–C(7a)–N(4)	108.6	107.9	108.0	107.8	107.7	107.4
C(1)–C(7a)–N(4)	106.6	106.9	107.0	107.3	110.0	110.3
O(3)–C(3)–N(4)	126.3	125.4	125.6	125.4	125.7	125.4
H(5)–C(5)–N(4)	121.3	121.2	121.4	121.5	121.2	121.4
H(6)–C(6)–C(5)	125.9	125.7	125.6	125.3	125.4	125.1
H(7)–C(7)–C(7a)	127.3	126.8	126.8	126.7	126.8	126.6
H(1)–C(1)–C(7a)	124.5	124.3	124.4	124.8	111.7	111.6
H(2)–C(2)–C(1)	128.7	128.7	128.5	128.4	113.1	113.1
H(1)–C(1)–C(7a)–N(4)	—	—	—	—	120.1	119.9
H(2)–C(2)–C(1)–C(7a)	—	—	—	—	119.2	119.0

than in the case of **1**. The values of the torsion angles, describing the out-of-plane positions of the hydrogen atoms on C(1) and C(2), display acceptable correspondence. The difference in C–H bond lengths between sp^2 and sp^3 hybridised carbon atoms amounts to about 0.01 Å, as expected.

Equally expected, the hydrogenation of the C(1)–C(2) bond on going from **1** to **2** has a profound effect on the bond lengths and angles in the saturated five-membered ring. The expected increase in length of the C(1)–C(2) bond is most pronounced, amounting to more than 0.18 Å at the MP2 level and more than 0.20 Å at the B3LYP/6-311+G* level. The neighbouring C(1)–C(7a) and C(2)–C(3) bonds also display elongation by about 0.045 Å and on average about 0.035 Å respectively. The C–O bond length remains virtually constant. Of the three C–N bonds the one involved in the amide [N(4)–C(3)], changes the most, shortening by about 0.03 Å, consistent with anti-aromatic behaviour in **1** (see below). Apart from the obvious changes from the sp^2 value (about 126° in a five-membered ring) to the sp^3 value (about 109°) in angles involving H(1) and H(2), the values of the rest of the valence angles also reflect the effect of the hydrogenation: while those in the pyrrole segment change by a negligible amount only, the values of the C(1)–C(7a)–N(4) and C(3)–N(4)–(7a) angles increase by about 3°. In contrast, the O(3)–C(3)–N(4) angle in the amide does not change. Overall, the agreement between the various calculations inspires confidence in the methodologies, which is to be expected for this kind of organic system, consisting of first row elements only.

Vibrational spectra

No vibrational spectroscopic data for **1** are available in the literature, except the carbonyl stretching frequency.[6] In order to obtain the most reliable estimates for the (perpendicular) amplitudes of vibration, it was deemed necessary to record the complete vibrational spectrum. An IR spectrum was recorded which showed most of the bands; nevertheless, a few intense bands were missing and a Raman spectrum was recorded to locate these. However, due to the particular electronic properties of pyrrolizin-3-one **1**, recording the Raman spectrum of a liquid film proved troublesome: the compound displayed fluorescence in the laser beam and due to an inconveniently large background, only an incomplete set of 15 bands was observed. Nevertheless, both spectra were combined into an almost complete set of frequencies, subsequently used to scale the theoretical vibrational frequencies: the νCH and the various νCC modes were scaled by 0.94, the νCO mode by 0.91 and the five δCH modes by 0.98. In the end an rms difference of 8 cm^{-1} and a largest difference of 19 cm^{-1} between calculated and experimental frequencies were obtained. Both the scaled calculated and experimental wavenumbers of **1** have been listed in Table 3. They demonstrate that there is a good agreement between the experiment and the calculations, in both the frequencies and the intensities of the signals.

An experimental vibrational spectrum of the dihydro compound **2** is also unavailable in the literature. However, based on the agreement between scaled calculated and experimental frequencies obtained for **1**, one can be confident in stating that a force field, obtained by the same computational method as in the case of **1** and scaled using the same scaling constants, is likely to reproduce the molecule's vibrational modes very accurately. In this case, all modes involving methylene groups (*i.e.* scissoring, rocking, wagging and twisting modes) were scaled down by 0.98. We list the scaled calculated frequencies in Table 4 for further reference.

GED model of pyrrolizin-3-one 1

Based on the results of the calculations a model was constructed in C_s symmetry requiring 21 parameters, but an extra parameter (p_{22}) was included to describe the butterfly motion of the molecule and to allow it to deviate from planarity. This 'butterfly' motion is defined as the folding along the line of the C–N bond joining the two rings.[17] The rest of the C–C and C–N bond distances were recombined in nine new independent parameters. Parameter p_1 describes the main feature of the radial-distribution curve and is defined as the mean of all C–C and C–N bond distances. Parameters p_2 to p_9 describe various means of and differences between groups of C–C and C–N distances. The five C–H distances in **1** were replaced by a single average distance [⟨*r*(C–H)⟩], which was combined with the C–O distance in two new independent parameters, *i.e.* the mean (p_{10}) and the difference parameter (p_{11}). From all these independent distances, the eleven separate bond distances were calculated as dependent parameters (p_{23} to p_{33} in Table 5, which lists all the parameters). The remaining independent parameters (p_{12} to p_{22}) are ten bond angles and the 'butterfly' angle.

Table 3 Observed and scaled calculated vibrational data for **1** (see text for scaling factors)[a]

$\nu_{calc.}$ ($I_{calc.}$)	$\nu_{exp.}$	$\nu_{calc.}$ ($I_{calc.}$)	$\nu_{exp.}$	$\nu_{calc.}$ ($I_{calc.}$)	$\nu_{exp.}$	$\nu_{calc.}$ ($I_{calc.}$)	$\nu_{exp.}$
3177 (1)		1406 (72)	1387 vs	997 (3)	998 m	685 (22)	683 s
3161 (0)		1389 (19)	1382 r	943 (2)	932 w	657 (14)	647 m
3153 (2)		1319 (6)	1313 w	915 (1)	900 w	618 (0)	633 r
3142 (3)		1249 (140)	1241 vs	878 (2)	870 w	593 (4)	582 s
3131 (5)	3130 m	1232 (25)	1224 r	828 (34)	820 s	549 (3)	548 s
1733 (520)	1731 vs	1154 (9)	1151 s	794 (23)	791 s	388 (2)	
1571 (45)	1569 s	1085 (20)	1087 s	752 (1)	752 r	304 (2)	
1528 (29)	1520 s	1051 (37)	1052 s	735 (47)	728 s	194 (6)	
1461 (31)	1463 s	1035 (9)	1032 m	707 (34)	706 s	125 (0)	

[a] Wavenumbers ν in cm^{-1} and intensities I in km mol^{-1}. w weak; m medium; s strong; vs very strong; r Raman band.

Table 4 Scaled calculated vibrational data for **2** (see text for scaling factors)[a]

$\nu_{calc.}$ ($I_{calc.}$)	$\nu_{calc.}$ ($I_{calc.}$)	$\nu_{calc.}$ ($I_{calc.}$)	$\nu_{calc.}$ ($I_{calc.}$)	$\nu_{calc.}$ ($I_{calc.}$)	$\nu_{calc.}$ ($I_{calc.}$)
3182 (2)	1742 (509)	1306 (34)	1075 (56)	833 (12)	614 (2)
3147 (3)	1570 (32)	1293 (199)	1024 (3)	790 (16)	543 (2)
3134 (6)	1497 (4)	1264 (15)	1022 (2)	723 (16)	525 (4)
3016 (7)	1466 (56)	1234 (0)	1005 (1)	717 (66)	309 (4)
2980 (8)	1459 (4)	1225 (3)	958 (1)	654 (31)	230 (7)
2978 (11)	1414 (62)	1165 (0)	913 (11)	635 (7)	136 (1)
2955 (31)	1410 (97)	1127 (10)	882 (0)	624 (1)	80 (2)

[a] Wavenumbers ν in cm^{-1} and intensities I in km mol^{-1}.

Table 5 Selected interatomic distances (r_a in Å) and amplitudes of vibration (u in Å) derived from the SARACEN study of pyrrolizin-3-one **1**

Atom pair	Distance	Amplitude	Atom pair	Distance	Amplitude
O(3)–C(3)	1.215(4)	0.040(4)	O(3)···C(6)	4.407(15)	0.086(8)
C(7a)–N(4)	1.377(7)	0.044(3)	C(3)···C(7)	3.500(7)	0.08(5)
C(3)–N(4)	1.434(4)	0.057(4)	C(3)···C(6)	3.658(13)	0.067(5)
H(5)–C(5)	1.087(4)	0.078(7)	C(2)···C(6)	4.309(10)	0.055(19)
O(3)···N(4)	2.343(10)	0.062(5)	H(2)···O(3)	2.876(22)	0.140(13)
O(3)···C(2)	2.479(10)	0.057(6)	H(1)···C(2)	2.188(13)	0.097(9)
C(6)···N(4)	2.269(13)	0.064(10)	H(6)···N(4)	3.305(12)	0.08(4)
C(7a)···C(6)	2.296(10)	0.055(5)	H(5)···C(3)	3.009(14)	0.136(13)
O(3)···C(5)	3.142(14)	0.093(9)	H(6)···O(3)	5.316(15)	0.119(12)
O(3)···C(7a)	3.467(7)	0.06(3)	H(5)···C(2)	4.297(11)	0.120(12)
C(3)···C(5)	2.614(8)	0.062(6)	H(2)···C(6)	5.374(10)	0.092(9)

GED structural refinement of pyrrolizin-3-one 1

Starting values for all parameters were taken from the MP2 calculation (the butterfly angle was fixed at 0°). When these values were compared with the experimental data at the beginning of the refinement procedure, an R factor of about 12% was obtained without refining any parameter or amplitude, which is an indication of the quality of both the calculations and the experimental data. In the end all independent parameters except for p_1, p_2, p_{11}, p_{12} and p_{13} were restrained, as were a number of the dependent parameters (p_{24}, p_{26}, p_{28}, p_{31}, p_{32} and p_{33}). This was necessary mainly because all bonded distances in the molecule are very similar and so many of the parameters involving C–C and C–N distances (p_3 to p_9) were ill-determined by the experimental data. The values for the restraints were based on the results of the various calculations and since these were in excellent agreement, the restraints on the different parameters are fairly tight. Once these were in place the values returned by the refinement lay well within the boundaries set by the restraints. Restraints were also applied to amplitudes of vibration that could not be refined independently. Values for the restraints were calculated directly from the scaled force field, with uncertainty ranges of 10% of the computed values for single amplitudes or 5% of the computed values for ratios of amplitudes. With these restraints in place, all amplitudes were refined. A full list of the restraints used in the refinements can be found in the supplementary data.

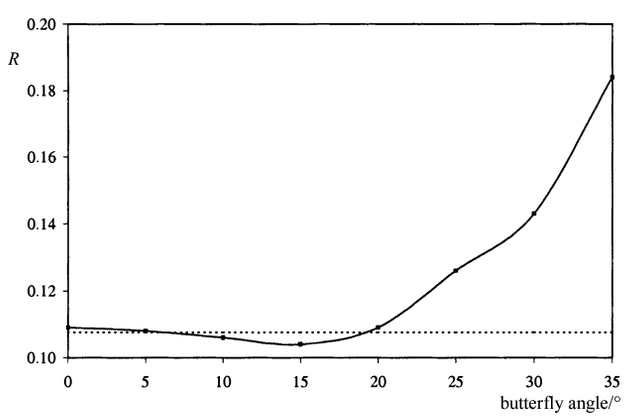

Fig. 3 Variation of the R factor with the value of the butterfly angle (p_{22}), in the refinement of the gas-phase structure of pyrrolizin-3-one **1**.

To investigate the planarity of the molecule, the butterfly angle (p_{22}) was fixed at various non-zero values and all remaining parameters for the resulting structures were completely refined. The R factors obtained in this way are graphically represented in Fig. 3. It shows that, in contrast to the planar geometry representing an energy minimum in the calculations, the data suggest that the two five-membered rings are inclined to one another by about 15°, even though the difference in R

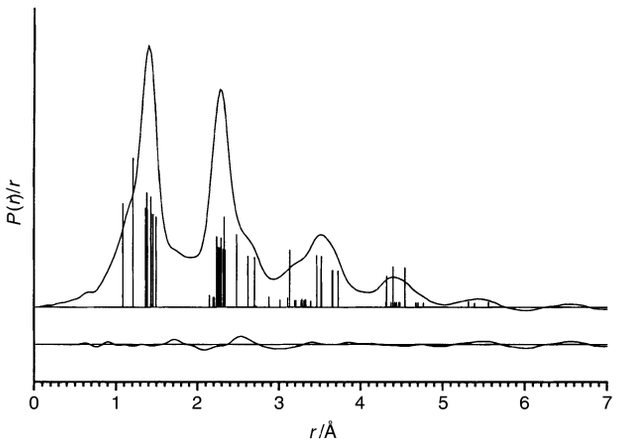

Fig. 4 Experimental and difference (experimental − theoretical) radial-distribution curves for pyrrolizin-3-one **1**. Before Fourier inversion the data were multiplied by $s\exp(-0.002s^2)/(Z_O - f_O)(Z_N - f_N)$.

factor is quite small and the changes in the values of the parameters were negligible. At a significance level of 0.005, given by the dashed line in Fig. 3, this would mean that the butterfly angle between the planes of the two five-membered rings lies somewhere between about 6 and 19°.[18] Note that the refined parameters are of the type r_{h1}, which indicates that vibrational effects (shrinkage) have already been taken into account. The final R_G factor for the refinement was 0.103. A lower value could be obtained if some restraints were released, but with such strongly correlated parameters, this procedure could lead to unrealistic values for the parameters. A selection of interatomic distance and vibrational amplitude values for the final structure is given in Table 5, and the final radial-distribution curve is shown in Fig. 4.

Table 6 shows good agreement between the experimental and theoretical data. Furthermore, for the MP2 calculation, all but four (p_1, p_{10}, p_{13} and p_{14}) independent parameters lie within one esd of the experimental values. Of these four exceptions, three of the values obtained in the MP2 calculation are closer to the experimental ones than the B3LYP values; p_{14} is unique since here the MP2 calculation overestimates the angle by about 2°, more than B3LYP. For the dependent parameters the difference between theory and experiment is slightly larger, most likely due to the fact that p_1 is underestimated by both methods: for MP2, half of the calculated values fall outside one esd of the GED value, but again this is a far better result than for B3LYP. Overall though, taking the esds on the experimental values into account, the differences are small and lie well below 0.01 Å.

Whether the fact that the experiment suggests non-planarity for **1** is an artefact of the refinement procedure (*i.e.* as a result of the harmonicity of the force field used) or a physical fact is difficult to assess. In any case, as is established by the force-field calculations, the molecule does display a low-frequency butterfly mode (125 cm^{-1}) and because of this the potential energy surface (PES) will be quite flat near the minimum, represented by the near-planar conformation. Consequently, taking in account the lowest vibrational mode, the calculations provide a reasonably accurate representation of the gas-phase structure of pyrrolizin-3-one **1**.

X-Ray structure and comparison with gas-phase geometry

Solid-state geometrical data for **1** and **2** are reported in Tables 7 and 8.§ The data for **1** are consistent with those reported for the 6-bromo-derivative **3**[2] but at an increased level of accuracy. The entire pyrrolizin-3-one molecule **1** is essentially planar (rms deviation of all heavy atoms 0.021 Å) but, more specifically, the two five-membered rings subtend a butterfly angle of 3.06(14)° about the N(4)–C(7a) bond. The corresponding figures for the azapyrrolizinones **4** and **5** are 2.5 and 4.2° respectively.[3] Compared with the gas-phase structures, therefore, the transition to the solid state apparently introduces packing effects which cause minor distortions in the rings and flatten the molecule to an almost coplanar arrangement. Surprisingly, the data suggest that the planarity of the dihydro-compound **2** is even more pronounced [rms deviation of heavy atoms 0.009 Å; butterfly angle of five-membered rings about the N(4)–C(7a) bond 1.14(9)°]. The bond lengths of the pyrrole ring [comprising N(4)–C(5)–C(6)–C(7)–C(7a)] of **1** and **2** are almost identical, within experimental error, but as expected, saturation of the C(1)–C(2) double bond causes an increase in the C(1)–C(7a), C(1)–C(2) and C(2)–C(3) distances in **2**. Both **1** and **2** display very large exocyclic bond angles at the ring junctions [C(3)–N(4)–C(5) 138.68(11) and 135.58(13)° respectively; C(1)–C(7a)–C(7) 145.23(13) and 142.92(13)° respectively], which are a characteristic feature of fused planar five-membered rings.[3]

Comparison of the geometries of the amide units [N(4)–C(3)–O(3)] of **1** and **2** is of particular interest. In both molecules, the delocalisation of the lone pair of the nitrogen atom is distributed between the π-systems of the pyrrole ring and of the amide unit. However, as shown in Scheme 1, amide-type delocalisation in **1** creates a formally anti-aromatic resonance structure **1a** not found with **2**/**2a**. This mode of electron distribution would therefore be expected to be relatively disfavoured in **1**, leading to C(3)–N(4) having less double bond character (*i.e.* being longer) and C(3)–O(3) having more double bond character (*i.e.* being shorter) than the corresponding parameters of **2**. The data in Tables 7 and 8 appear to lend support to this interpretation, notwithstanding the fact that the C=O bond length in amides is rather insensitive to structural variation.[19] Thus, for **2**, the appropriate C–N bond [1.392(2) Å] is significantly shorter than the corresponding bond in **1** [1.408(2) Å] and this trend is further borne out by the MP2 calculations (Tables 7 and 8). The XRD figures for the C=O distances [**1** 1.207(2) Å; **2** 1.216(2) Å] provide further support—though at the limit of accuracy of the data, and not confirmed by the calculations. Finally, it must be emphasised that the amide geometries of both **1** and **2** are grossly atypical by comparison with those of other cyclic tertiary amides [C–N 1.335(9) Å; C=O 1.234(11) Å].[19] This is associated with the *N*-acylpyrrole substructure, and we have already commented on similar features of the *N*-acylimidazole derivatives **4** and **5**.[3] The unusual amide geometry also accounts for the infra-red carbonyl stretch of **1** (1731 cm^{-1}, Table 3), which occurs at an unexpectedly high frequency for an amide.

From Tables 7 and 8, which list the heavy-atom structural parameters obtained in the analyses, it is clear that the changes on going from the gas phase to the solid are minimal. In the case of **1**, most of the distance parameters that do change get smaller in the solid: C(7)–C(7a), C(5)–C(6) and N(4)–C(3) shorten by about 0.03 Å, while the changes in C(1)–C(2) and C(2)–C(3) are smaller and amount to about 0.02 and 0.01 Å, respectively. The agreement between gas and solid regarding the angles is even more convincing, the changes being limited to less than 2°. Compound **2** displays similar changes on going to the condensed phase, even though they are generally smaller: C(7)–C(7a) shortens by about 0.03 Å, as in **1**, but C(5)–C(6), N(4)–C(3) and C(2)–C(3) by only 0.02, 0.015 and 0.01 Å, respectively. These apparent contractions reflect the different physical meanings of distances determined by electron and X-ray diffraction in gas and solid phases respectively. Equally, taking the esds on the experimental values into account, the differences in the angles are small, amounting to no more than about 1°.

§ CCDC reference numbers 161065 and 168077. See http://www.rsc.org/suppdata/p2/b1/b102475m/ for crystallographic files in .cif or other electronic format.

Table 6 Experimental geometrical parameters from the SARACEN gas-phase study of pyrrolizin-3-one **1** (r_{h1} distances in Å and angles in °). For definition of parameters and details of the refinement, see text. Values in parentheses are esds obtained in the least-squares refinement

	Parameter	GED	B3LYP[a]	MP2[b]
Independent				
p_1	Av. of *r*(C–C) and *r*(C–N)	1.4176(10)	1.4088	1.4125
p_2	Av. of *r*[C(6)–C(7)], *r*[C(1)–C(7a)], *r*[C(2)–C(3)] and *r*[C(3)–N(4)] − av. of *r*[C(7)–C(7a)], *r*[C(5)–C(6)], *r*[C(1)–C(2)], *r*[C(5)–N(4)] and *r*[C(7a)–N(4)]	0.074(4)	0.0819	0.0768
p_3	*r*[C(2)–C(3)] − av. of *r*[C(6)–C(7)], *r*[C(7a)–C(1)] and *r*[C(3)–N(4)]	0.0525(19)	0.0504	0.0519
p_4	*r*[C(7a)–C(1)] − av. of *r*[C(6)–C(7)] and *r*[C(3)–N(4)]	0.023(4)	0.0205	0.0243
p_5	*r*[C(6)–C(7)] − *r*[C(3)–N(4)]	0.002(6)	0.0096	0.0043
p_6	Av. of *r*[C(7)–C(7a)], *r*[C(5)–C(6)] and *r*[C(5)–N(4)] − av. of *r*[C(1)–C(2)] and *r*[C(7a)–N(4)]	0.021(9)	0.0108	0.0166
p_7	*r*[C(7)–C(7a)] − av. of *r*[C(5)–C(6)] and *r*[C(5)–N(4)]	0.003(5)	−0.0027	0.0037
p_8	*r*[C(5)–C(6)] − *r*[C(5)–N(4)]	0.005(9)	−0.0077	0.0050
p_9	*r*[C(1)–C(2)] − *r*[C(7a)–N(4)]	−0.017(14)	−0.0288	−0.0158
p_{10}	Av. of ⟨*r*(C–H)⟩ and *r*[C(3)–O(3)]	1.153(3)	1.1437	1.1480
p_{11}	⟨*r*(C–H)⟩ − *r*[C(3)–O(3)]	−0.125(6)	−0.1218	−0.1236
p_{12}	H(5)–C(5)–N(4)	121.5(5)	121.4	121.5
p_{13}	O(3)–C(3)–N(4)	124.4(9)	125.6	125.4
p_{14}	C(5)–N(4)–C(7a)	108.7(7)	110.1	110.6
p_{15}	C(3)–N(4)–C(7a)	111.17(10)	111.06	111.16
p_{16}	C(7)–C(7a)–N(4)	107.7(4)	108.0	107.8
p_{17}	C(1)–C(7a)–N(4)	107.6(4)	107.0	107.3
p_{18}	H(7)–C(7)–C(7a)	126.73(10)	126.83	126.73
p_{19}	H(1)–C(1)–C(7a)	124.9(5)	124.4	124.8
p_{20}	H(6)–C(6)–C(5)	125.4(5)	125.6	125.3
p_{21}	H(2)–C(2)–C(1)	128.5(5)	128.5	128.4
p_{22}	Butterfly angle	15.0 f[c]	0.0	0.0
Dependent				
p_{23}	C(7)–C(7a)	1.395(5)	1.3750	1.3875
p_{24}	C(6)–C(7)	1.439(4)	1.4397	1.4362
p_{25}	C(5)–C(6)	1.394(7)	1.3738	1.3863
p_{26}	C(7a)–C(1)	1.461(3)	1.4554	1.4584
p_{27}	C(1)–C(2)	1.363(10)	1.3516	1.3605
p_{28}	C(2)–C(3)	1.498(3)	1.4921	1.4941
p_{29}	N(4)–C(5)	1.389(7)	1.3815	1.3813
p_{30}	N(4)–C(7a)	1.380(7)	1.3804	1.3763
p_{31}	N(4)–C(3)	1.437(4)	1.4301	1.4319
p_{32}	⟨C–H⟩	1.090(4)	1.0828	1.0862
p_{33}	C(3)–O(3)	1.215(4)	1.2046	1.2098

[a] Refers to the B3LYP/6-311+G* (6-31G* on H) calculation. [b] Refers to the MP2/6-311+G* (6-31G* on H) calculation. [c] f indicates that the parameter was kept fixed (see text for details).

Table 7 Selected data comparing solid-state (XRD), experimental gas-phase (GED, r_{h1}) and calculated gas-phase (MP2, r_e) geometries for **1**; bond lengths in Å and angles in °

Parameter	XRD	GED	MP2
C(7)–C(7a)	1.364(2)	1.395(5)	1.3875
C(6)–C(7)	1.437(2)	1.439(4)	1.4362
C(5)–C(6)	1.365(2)	1.394(7)	1.3863
C(1)–C(7a)	1.457(2)	1.461(3)	1.4584
C(1)–C(2)	1.344(2)	1.363(10)	1.3605
C(2)–C(3)	1.489(2)	1.498(3)	1.4941
N(4)–C(5)	1.384(2)	1.389(7)	1.3813
N(4)–C(7a)	1.381(2)	1.380(7)	1.3763
N(4)–C(3)	1.408(2)	1.437(4)	1.4319
C(3)–O(3)	1.207(2)	1.215(4)	1.2098
O(3)–C(3)–N(4)	125.22(12)	124.4(9)	125.4
C(5)–N(4)–C(7a)	110.03(10)	108.7(7)	110.6
C(3)–N(4)–C(5)	138.68(11)	137.5(6)	138.2
C(3)–N(4)–C(7a)	111.13(10)	111.17(10)	111.16
C(7)–C(7a)–N(4)	107.85(11)	107.7(4)	107.8
C(1)–C(7a)–N(4)	106.85(10)	107.6(4)	107.3
C(1)–C(7a)–C(7)	145.23(13)	141.8(6)	144.9

Table 8 Selected data comparing solid-state (XRD) and calculated gas-phase (MP2) geometries for **2**; bond lengths in Å and angles in °

Parameter	XRD	MP2
C(7)–C(7a)	1.358(2)	1.3800
C(6)–C(7)	1.437(2)	1.4367
C(5)–C(6)	1.363(2)	1.3847
C(1)–C(7a)	1.502(2)	1.5033
C(1)–C(2)	1.545(2)	1.5479
C(2)–C(3)	1.515(2)	1.5268
N(4)–C(5)	1.387(2)	1.3801
N(4)–C(7a)	1.390(2)	1.3846
N(4)–C(3)	1.392(2)	1.4068
C(3)–O(3)	1.216(2)	1.2095
O(3)–C(3)–N(4)	124.35(13)	125.4
C(5)–N(4)–C(7a)	110.62(12)	111.0
C(3)–N(4)–C(5)	135.58(13)	135.4
C(3)–N(4)–C(7a)	113.76(11)	113.7
C(7)–C(7a)–N(4)	107.34(12)	107.4
C(1)–C(7a)–N(4)	109.71(12)	110.3
C(1)–C(7a)–C(7)	142.92(13)	142.3

In the packing scheme for pyrrolizin-3-one **1**, molecules related by inversion centres are linked by pairwise C–H···O interactions characterised by an H···O distance of 2.44(2) Å and a C–H···O angle of 158(2)° (Fig. 5). Each molecule also lies 3.679(2) Å from a neighbouring molecule related to it by another inversion centre, suggesting the presence of slight π–π interactions. These interactions together give zigzag chains of molecules running parallel to the crystallographic *b*-axis. In the packing of 1,2-dihydropyrrolizin-3-one **2** the molecules are packed in bilayers generated through C–H···O contacts, which are indicated by dashed lines in Fig. 6. Each O atom participates in two such contacts: the O···H distances are 2.46(2) and 2.50(2) Å and the corresponding C–H···O angles are 165(2) and 170(2)°. The perpendicular distance between adjacent pairs of molecules has lengthened to 3.824(2) Å and is therefore not considered to represent a significant interaction.

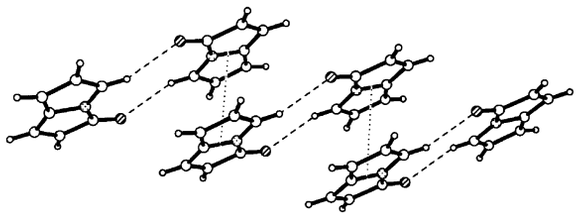

Fig. 5 A view of the intermolecular interactions in pyrrolizin-3-one **1**. Dashed lines indicate C–H · · · O contacts and dotted lines the direction of B–B interactions, where B is the mid-point of the N(4)–C(7a) bond. These interactions link molecules into zigzag chains running parallel to *b*. Atoms are identified as follows: H small plain circles, C large plain circles, N regular dot pattern, O shaded.

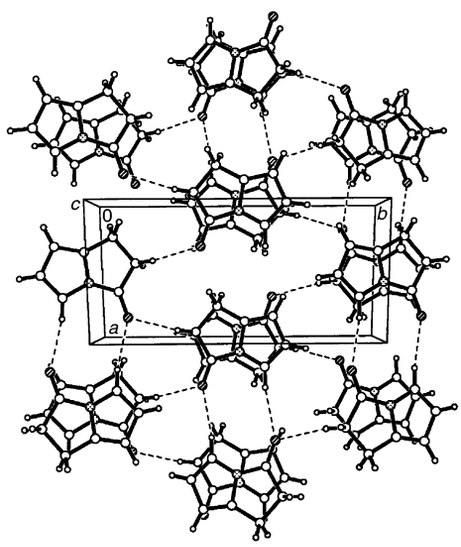

Fig. 6 A view of the packing of molecules of **2** along the *c*-axis, showing the bilayers indicated by dashed lines. Atoms are identified as follows: H small plain circles, C large plain circles, N regular dot pattern, O shaded.

Conclusion

The work described in this paper provides definitive structural information for the pyrrolizin-3-one system **1** both in the solid state and in the gas phase. There are few significant differences in the data, as measured by XRD and GED or calculated by *ab initio* methods. The system is essentially planar with considerable distortion of the exocyclic bond angles at the bridgehead from the 120° value expected for sp^2 hybridised atoms. The geometry of the amide unit is also unusual: in particular, the length of the C–N bond is much longer than for typical amides. Comparison of this feature of the structure with the corresponding data for the 1,2-dihydro compound **2** indicates that a component of the bond lengthening may be due to the reluctance of the system to create an anti-aromatic 8π unit by delocalisation.

Acknowledgements

We are indebted to the EPSRC for financial support of the Edinburgh Electron Diffraction Service (grant GR/K44411) and for the provision of an X-ray diffractometer. We also thank Dr Lise Hedberg (Oregon State University) for providing a copy of the ASYM40 program, and Dr V. A. Sipachev (Moscow State University) for providing us with a copy of the program SHRINK[15] and for his assistance in its use.

References

1 H. McNab and C. Thornley, *Heterocycles*, 1994, **37**, 1977.
2 A. J. Blake, H. McNab and R. Morrison, *J. Chem. Soc., Perkin Trans. 1*, 1988, 2145.
3 A. J. Blake, H. McNab and C. Thornley, *J. Chem. Res. (S)*, 1997, 238; A. J. Blake, H. McNab and C. Thornley, *J. Chem. Res. (M)*, 1997, 1615.
4 A. J. Blake, P. T. Brain, H. McNab, J. Miller, C. A. Morrison, S. Parsons, S. D. W. H. Rankin, H. E. Robertson and B. A. Smart, *J. Phys. Chem.*, 1996, **100**, 12280; P. T. Brain, C. A. Morrison, S. Parsons and D. W. H. Rankin, *J. Chem. Soc., Dalton Trans.*, 1996, 4589.
5 H. McNab, *J. Org. Chem.*, 1981, **46**, 2809.
6 W. Flitsch and U. Neumann, *Chem. Ber.*, 1971, **104**, 2170.
7 C. M. Huntley, G. S. Laurenson and D. W. H. Rankin, *J. Chem. Soc., Dalton Trans.*, 1980, 954.
8 J. R. Lewis, P. T. Brain and D. W. H. Rankin, *Spectrum*, 1997, **15**, 7.
9 A. W. Ross, M. Fink and R. Hilderbrandt, in *International Tables for Crystallography*, ed. A. J. C. Wilson, Kluwer Academic Publishers, Dordrecht, 1992, vol. C, p. 245.
10 J. Cosier and A. M. Glazer, *J. Appl. Crystallogr.*, 1986, **19**, 105.
11 Gaussian 98, Revision A.7, M. J. Frisch, G. W. Trucks, H. B. Schlegel, G. E. Scuseria, M. A. Robb, J. R. Cheeseman, V. G. Zakrzewski, J. A. Montgomery, Jr., R. E. Stratmann, J. C. Burant, S. Dapprich, J. M. Millam, A. D. Daniels, K. N. Kudin, M. C. Strain, O. Farkas, J. Tomasi, V. Barone, M. Cossi, R. Cammi, B. Mennucci, C. Pomelli, C. Adamo, S. Clifford, J. Ochterski, G. A. Petersson, P. Y. Ayala, Q. Cui, K. Morokuma, D. K. Malick, A. D. Rabuck, K. Raghavachari, J. B. Foresman, J. Cioslowski, J. V. Ortiz, A. G. Baboul, B. B. Stefanov, G. Liu, A. Liashenko, P. Piskorz, I. Komaromi, R. Gomperts, R. L. Martin, D. J. Fox, T. Keith, M. A. Al-Laham, C. Y. Peng, A. Nanayakkara, C. Gonzalez, M. Challacombe, P. M. W. Gill, B. Johnson, W. Chen, M. W. Wong, J. L. Andres, M. Head-Gordon, E. S. Replogle and J. A. Pople, Gaussian, Inc., Pittsburgh PA, 1998.
12 J. S. Binkley, J. A. Pople and W. J. Hehre, *J. Am. Chem. Soc.*, 1980, **102**, 939; M. S. Gordon, J. S. Binkley, J. A. Pople, W. J. Pietro and W. J. Hehre, *J. Am. Chem. Soc.*, 1982, **104**, 2797; W. J. Pietro, M. M. Francl, W. J. Hehre, D. J. Defrees, J. A. Pople and J. S. Binkley, *J. Am. Chem. Soc.*, 1982, **104**, 5039.
13 W. J. Hehre, R. Ditchfield and J. A. Pople, *J. Chem. Phys.*, 1973, **56**, 2257; P. C. Hariharan and J. A. Pople, *Mol. Phys.*, 1974, **27**, 209; M. S. Gordon, *Chem. Phys. Lett.*, 1980, **76**, 163.
14 A. D. McLean and G. S. Chandler, *J. Chem. Phys.*, 1980, **72**, 5639; R. Krishnan, J. S. Binkley, R. Seeger and J. A. Pople, *J. Chem. Phys.*, 1980, **72**, 650.
15 ASYM40 version 3.0, update of ASYM20; L. Hedberg and I. M. Mills, *J. Mol. Spectrosc.*, 1993, **160**, 117.
16 V. A. Sipachev, *J. Mol. Struct. (THEOCHEM)*, 1985, **121**, 143; V. A. Sipachev, in *Advances in Molecular Structure Research*, eds. I. Hargittai and M. Hargittai, JAI Press, Greenwich, 1999, vol. 5, p. 263.
17 P. Pulay, G. Fogorasi, F. Pang and J. E. Boggs, *J. Am. Chem. Soc.*, 1979, **101**, 2550; G. Fogorasi, X. Zhou, P. W. Taylor and P. Pulay, *J. Am. Chem. Soc.*, 1992, **114**, 8191.
18 W. C. Hamilton, *Acta Crystallogr.*, 1965, **18**, 502.
19 P. Chakrabarti and J. D. Dunitz, *Helv. Chim. Acta*, 1982, **65**, 1555.